Tunable Acoustic Superscattering for Subwavelength Structure

Long Sun and Ying Wu

Division of Computer, Electrical and Mathematical Science and Engineering,
King Abdullah University of Science and Technology

King Abdullah University of Science and Technology

Abu Dhabi 2025 PIERS THE ELECTROMAGNETICS ACADEMY

BACKGROUND

Superscattering, which greatly enhances the interaction between waves and matter, plays a crucial role in wave manipulation across acoustics and optics. The scattering intensity of superscattering significantly exceeds the conventional limit, characterized by the far-field spreading pattern in field distribution.

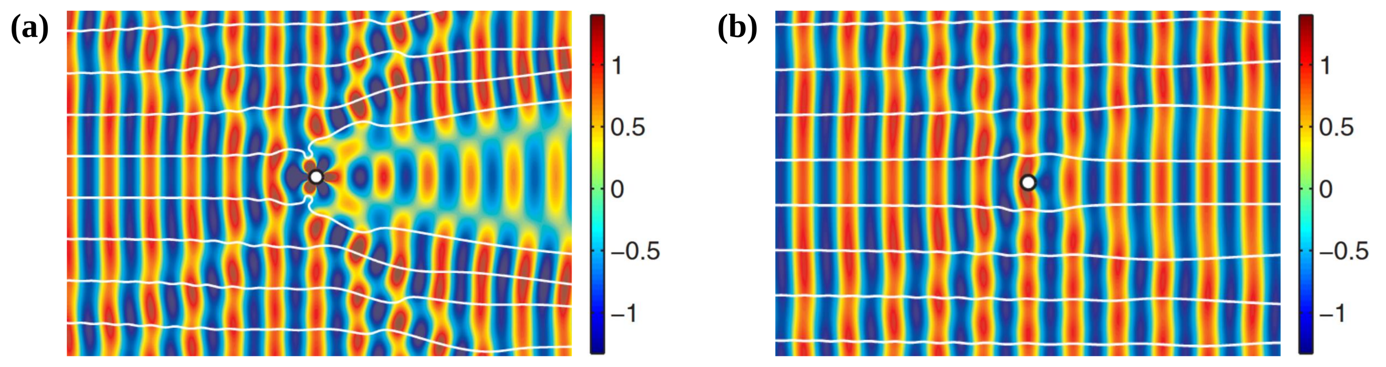

FIG 1, Field distribution of (a) superscattering[1] and (b) normal scattering.

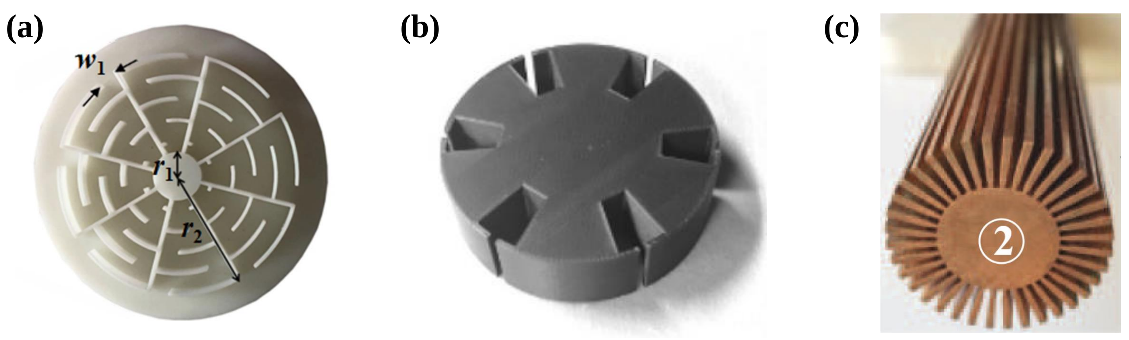

FIG 2, Figures of (a) coiling-up space [2], (b) Helmholtz resonator [3] and (c) corrugated cylinder [4].

In acoustic superscattering, the main challenge is the complex design and limited tunability of the superscatterer, which constrain the phenomenon to narrow frequency bands. Therefore, the tunable superscattering which could broaden the operational frequency range is needed for diverse applications.

ANISOTROPIC MODEL

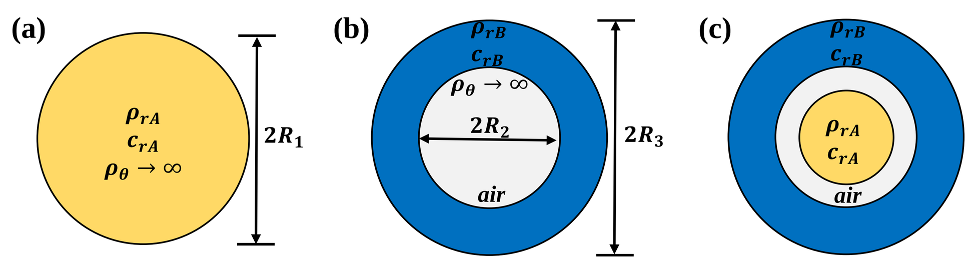

FIG 3, Schematic of (a) circular, (b) annular and (c) composite scatterer.

The materials are characterized by radial sound speed c_r, radial mass density ρ_r, and azimuthal mass density ρ_θ. The impedance $\sqrt{c_r \rho_r}$ of each scatterer is matched to the surrounding air, ensuring efficient wave coupling and enhanced acoustic scattering.

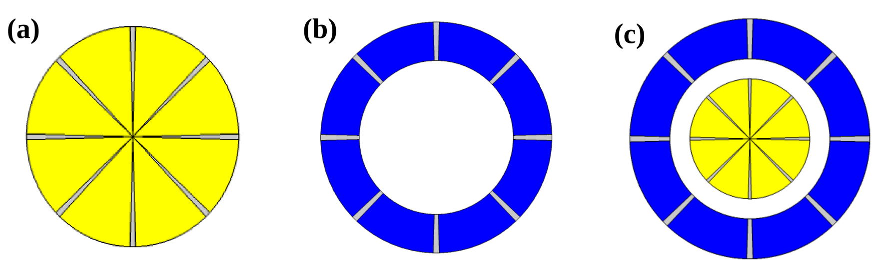

FIG 4, Realization of anisotropy for (a) circular, (b) annular and (c) composite scatterer.

The anisotropy is realized by hard wall slits separating the material, which results in extreme azimuthal mass density.

SUPERSCATTERING MECHANISM

We use **Mie scattering theory** in anisotropic media to analyze the model[5]. The general expression for the pressure field is:

$$p(r,\theta) = \sum_{m=-\infty}^{\infty} [a_m J_v(k_r r) + b_m H_v^{(1)}(k_r r)] e^{im\theta},$$

where $v = m\sqrt{\rho_r/\rho_\theta}$, which related to anisotropy. In extreme anisotropic medium, the high-order terms are suppressed, causing $v \to 0$, which significantly alters the scattering behavior. Consider an anisotropic circular scatterer under plane wave incidence, we express the pressure field inside and outside the scatterer respectively:

$$p_1(r,\theta) = \sum_{m=-\infty}^{\infty} A_m J_0(k_r r) e^{im\theta},$$

$$p_2(r,\theta) = \sum_{m=-\infty}^{\infty} [i^m J_m(k_0 r) + D_m H_m^{(1)}(k_0 r)] e^{im\theta},$$

Applying the boundary conditions for pressure and velocity continuity, we derive the scattering coefficients :

$$D_m = \frac{J_m(k_0 R_1) J_0'(k_r R_1) - J_m'(k_0 R_1) J_0(k_r R_1)}{H_m^{(1)\prime}(k_0 R_1) J_0(k_r R_1) - H_m^{(1)}(k_0 R_1) J_0'(k_r R_1)},$$

the anisotropy forces multipole modes to degenerate at lower frequencies, leading to constructive interference and thus total scattering cross-section $D = \frac{4}{k_0}\sum_{m=-\infty}^{\infty}|D_m|^2$ exceeds the single-channel limit.

SCATTERING CHARACTERISTIC

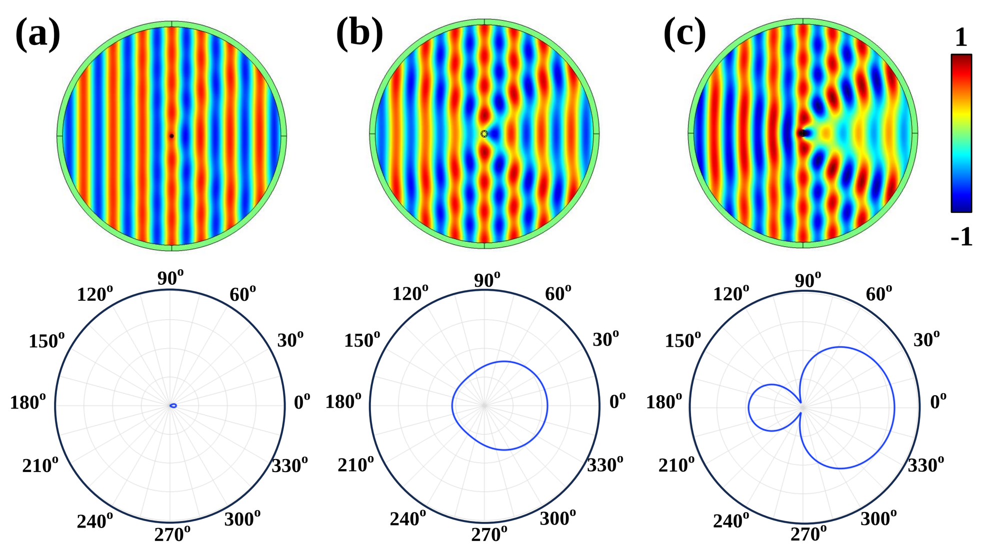

FIG 5, Pressure field and far-field distribution of models in FIG 4 with R_1=7.5*cm*, R_2=10*cm* and R_3=15*cm* at f=268 Hz with n_A=4 and n_B=5.

Across the pressure field distributions, the composite scatterer exhibits significantly enhanced scattering compared to individual circular or annular scatterers. The superscattering is valid for the composite structure.

The far-field radiation pattern of composite scatterer highlights the **directional scattering intensity**, compared with the weak scattering of circular scatter and the uniform scattering of annular scatterer.

TUNABLE SUPERSCATTERING

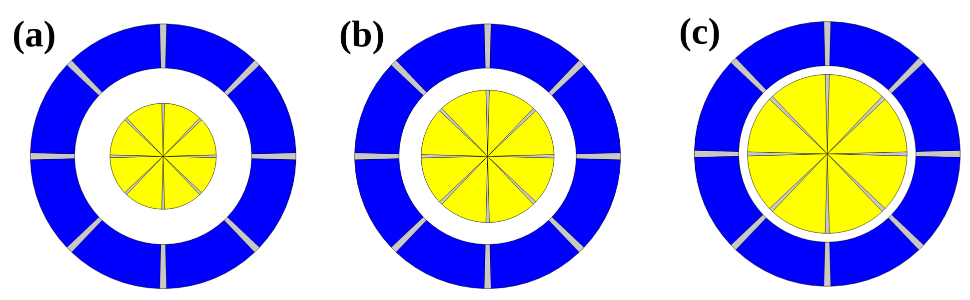

FIG 6, Tunable Superscatterers with air thicknesses of (a) t = 4 cm, (b) t = 2.5 cm and (c) t = 1 cm with n_A=4 and n_B=5.

The tunable superscattering is achieved by changing the air layer thickness. The reduced speed c_{rA} of the circular scatterer inside the cavity, which is significantly lower than the background air speed c_0, **enables the superscattering to occur at low frequencies**.

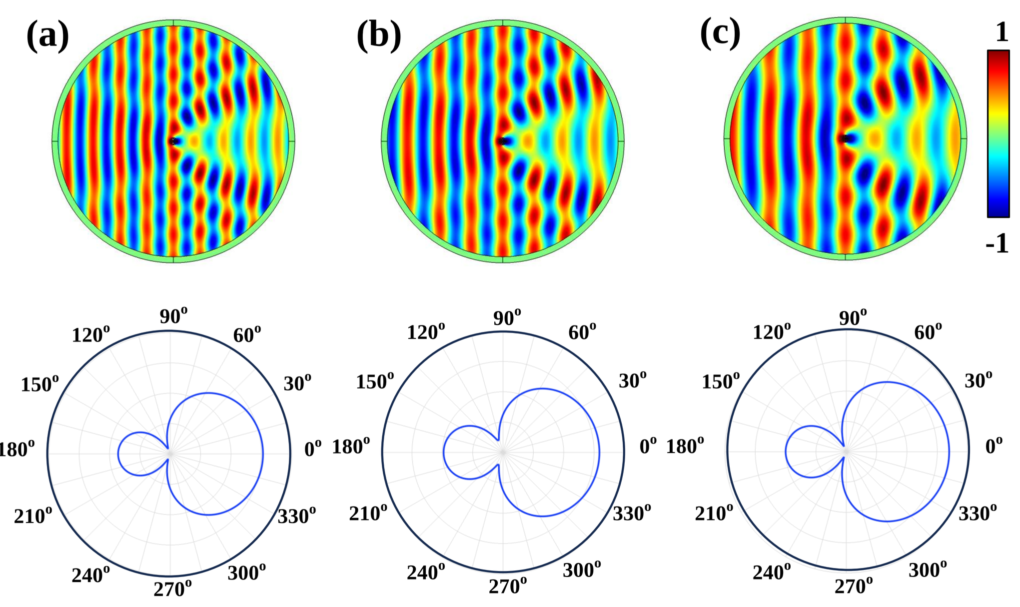

FIG 7, Pressure field and far-field distribution of (a) t =4 cm, f =314 Hz, (b) t =2.5 cm, f =265 Hz and (c) t =1 cm, f =221 Hz.

The pressure field distribution and far-field pattern of tunable scatterers all show the superscattering phenomenon, which **validates the tunability and effectiveness** of the design.

In FIG 8, superscattering can be obtained across a broad frequency range. Results indicate that thinner air layers lead to lower resonance frequencies, enabling precise control over scattering behavior for specific application.

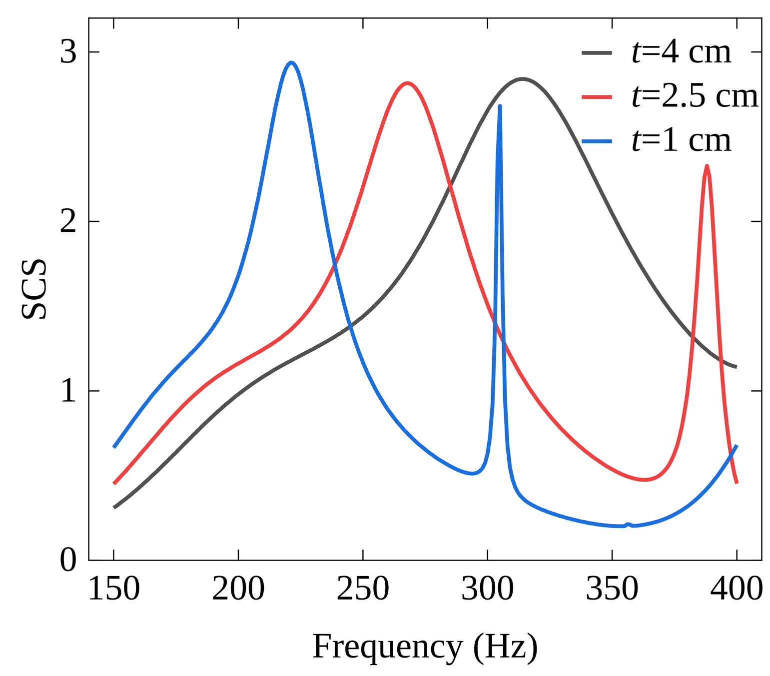

FIG 8, Normalized total SCSs calculated from different thicknesses t of all the composite scatters above.

CONCLUSION

Main Contributions:

- Tunable acoustic superscatterer
- Anisotropic Mie scattering theory
- Dynamic broadband superscattering

OUTLOOK

Possible Applications:

- Ultrasound diagnostics: Improved imaging resolution
- Underwater communication: Enhanced frequency range
- Architectural acoustics: Optimized sound control

ACKNOWLEDGEMENT

The work is supported by Office of the Sponsored Research (OSR) at King Abdullah University of Science and Technology (KAUST) under grant No. ORFS-CRG11-2022-5055, ORFS-OFP-2023-5560, and BAS/01/1626-01-01

References

1. Ruan, Z., & Fan, S., "Superscattering of light from subwavelength nanostructures," *Physical review letters*, Vol. *105*, No. 1, 013901, 2010.
2. Liu, F., Zhang, S., Luo, L., Li, W., Wang, Z. & Ke, M., "Superscattering of sound by a deep-subwavelength solid mazelike rod," *Physical Review Applied*, Vol. *12*, No. 6, 064063 2019.
3. Lee, T., Nomura, T., Schmalenberg, P., Dede, E.M., & Iizuka, H., "Directional acoustic superscattering by coupled resonators," *Physical Review Applied*, Vol. *12*, No. 5, 054059, 2019.
4. Shcherbinin, V.I., Fesenko, V.I., Tkachova, T.I. and Tuz, V.R., "Superscattering from subwavelength corrugated cylinders," *Physical Review Applied*, Vol. *13*, No. 2, 024081. 2020.
5. Zhao, J., Zhang, L., &Wu Y., "Enhancing monochromatic multipole emission by a subwavelength enclosure of degenerate Mie resonances," *The Journal of the Acoustical Society of America*, Vol. *142*, No 1, EL24-EL29, 2017.